WATER RESOURCES RESEARCH, VOL. 34, NO. 8, PAGES 1865–1879, AUGUST, 1998

Unsaturated zone processes and the hydrologic response of a steep, unchanneled catchment

Raymond Torres,[1] William E. Dietrich,[2] David R. Montgomery,[3]
Suzanne P. Anderson,[4] and Keith Loague[5]

Abstract. As part of a larger, collaborative study, we conducted field experiments to investigate how rainfall signals propagate through an unsaturated soil profile, leading to a rapid pore pressure response and slope instability. We sprinkler-irrigated an entire, unchanneled headwater basin in the steep, humid Oregon Coast Range, and we drove the system to quasi steady state as indicated by tensiometers, piezometers, and discharge. During initial wetting some of the deeper tensiometers responded before the arrival of an advancing head gradient front. With continued irrigation most tensiometers attained near-zero pressure heads before most piezometers responded fully, and a stable unsaturated flow field preceded the development of a stable saturated flow field. Steady discharge occurred after the last piezometer reached steady state. With the onset of steady discharge the unsaturated zone, saturated zone, and discharge became delicately linked, and a spike increase in rain intensity led to a response in the saturated zone and discharge much faster than could have happened through advection alone. We propose that the rain spike produced a slight pressure wave that traveled relatively rapidly through the unsaturated zone, where it caused a large change in hydraulic conductivity and the rapid effusion of stored soil water. An important control on the hydrologic response of this catchment lies with the soil-water retention curve. In general, below pressure heads of about -0.05 m, soil-water contents change slightly with changes in pressure head, but above -0.05 m the soil-water content is highly variable. Minor rainstorms upon a wet soil can produce slight changes in pressure head and corresponding large changes in soil-water content, giving rise to the passage of pressure waves in response to increased rain intensity and a relatively rapid response in the unsaturated zone. This rapid unsaturated zone response led to a rapid rise in the saturated zone, and it may be the underlying mechanism enabling short bursts of rain to cause slope instability.

1. Introduction

High infiltration capacities associated with the shallow soil mantle of steep, humid headwater basins and the presence of less permeable bedrock at depth create conditions that favor shallow subsurface storm flow [e.g., *Dunne*, 1978; *Pierson*, 1980]. Typically, rainwater and snowmelt permeate the soil and subsoil under gravity and capillary forces to an underlying less permeable zone. The permeability contrast leads to the development of a perched saturated zone, and downslope saturated flow ensues. In regions where shallow subsurface storm flow is the dominant means by which water reaches the channel (e.g., the steep coastal mountains of the Pacific Northwest) all incident precipitation must pass through a largely unsaturated soil profile before contributing to runoff. Hence unsaturated zone processes may directly control the timing and magnitude of positive pore pressure development and peak discharge.

Flow through the unsaturated zone is assigned variable importance in digital terrain based hydrologic models used to examine the spatial variability of runoff across landscapes. Generally, these models either ignore unsaturated flow (e.g., *Iida* [1984], TOPOG [*O'Loughlin*, 1986], and TAPES [*Moore et al*., 1988]) or assume it occurs as vertical flow equal to the rainfall rate (e.g., TOPMODEL [*Beven and Kirkby*, 1979]). These assumptions are particularly important when applied to steep landscapes, where such hydrologic models have formed the basis for predicting the spatial distribution and timing of shallow landslides [e.g., *Okimura and Kawatani*, 1987; *Dietrich et al*., 1992, 1993, 1995; *Montgomery and Dietrich*, 1994; *Hsu*, 1994; *Wu and Sidle*, 1995]. Such landslides typically occur in response to intense rainstorms, and pressure lags created by passage of precipitation through the unsaturated zone may greatly affect the hydrologic conditions necessary to generate slope instability. While some coupled hydrologic and slope stability models may be able to locate areas most likely to fail during a heavy rainstorm, they have limited ability to specify the magnitude and duration of the destabilizing rainstorms. In particular, they do not address the problem of how rapid pore pressure and discharge responses can occur through an unsaturated soil profile.

In field and laboratory studies, rapid unsaturated zone processes like macropore flow [e.g., *Mosley*, 1979, 1982;

[1]Department of Geological Sciences, University of South Carolina, Columbia.
[2]Department of Geology and Geophysics, University of California, Berkeley.
[3]Department of Geological Sciences, University of Washington, Seattle.
[4]Department of Earth Sciences and Institute of Tectonics, University of California, Santa Cruz.
[5]Department of Geological and Environmental Sciences, Stanford University, Stanford, California.

Paper number 98WR01140.
0043-1397/98/98WR-01140$09.00

Tsuboyama et al., 1994], fingering [e.g., *Hill and Parlange*, 1972; *Hendrickx et al*., 1993; *Glass and Nichol*, 1996], traveling waves [e.g., *Zimmermann et al*., 1966; *Andersen and Sevel*, 1974; *Smith*, 1977; *Gilham*, 1984; *Kayane and Kaihotsu*, 1988; *Novakowski and Gilham*, 1988; *Marui et al*., 1993], and preferential flow through well connected "mesopores" [e.g., *Wilson and Luxmoore*, 1988] were detected, and in each case it was recognized that rapid advection of water will have local effects on water table height, solute transport, and catchment runoff. However, conditions favoring the development and recurrence of rapid unsaturated zone processes remain poorly defined.

Another enigmatic hydrologic process is that of downslope unsaturated flow. Theoretical studies suggest that lateral unsaturated flow may arise from soil anisotropy [e.g., *Zaslavsky and Rogowski*, 1969; *Zaslavsky and Sinai*, 1981a, b] or from state dependent anisotropy [e.g., *McCord et al*., 1991]. However, *Philip* [1991] showed that a time dependent downslope flow component results from the downslope component of gravity. Equipotential fields that would give rise to downslope unsaturated flow paths were depicted in the numerical simulations of *Freeze* [1972], although he did not discuss this finding. *Humphrey* [1983] simulated pore pressure response to rainfall in a steep hollow that was mantled with highly permeable soil. Humphrey's three-dimensional (3-D) results show that unsaturated flow paths were unaffected by topographic convergence and were everywhere vertical except very near a water table or at the bedrock boundary.

Field studies of water flow through sloping soils led researchers to suggest that lateral unsaturated flow contributes to storm flow [e.g., *Hewlett and Hibbert*, 1967; *Weyman*, 1973; *Harr*, 1977; *McDonnell*, 1990; *Wilson et al*., 1991], and it may also serve to sustain base flow [e.g., *Hewlett and Hibbert*, 1963; *Hewlett*, 1969]. *Harr* [1977] conducted a field study designed to evaluate runoff generation from a steep hillslope mantled with highly permeable soils. On the basis of the work of *Zaslavsky and Rogowski* [1969], Harr divided unsaturated flux into slope parallel and vertical components, and he calculated their respective values. Harr found that slight changes in unsaturated pressure head could cause large changes in the unsaturated flux magnitude and direction, and he argued that lateral unsaturated flow plays an important role in generating high pore pressures and the discharge response. Field data documenting the slope parallel component were lacking, however, and his analysis was biased in favor of slope parallel flow. From a field site at the Maimai catchment, New Zealand, *McDonnell* [1990] depicted slope parallel unsaturated flow paths down to a depth of ~3 m, and they were sustained for an entire storm cycle [see *McDonnell*, 1990, Figure 8]. This interpretation, however, was an artifact of the vertical exaggeration of the illustration; without it the flow paths were predominantly vertical. Hence results from theoretical, numerical, and field studies reveal considerable uncertainty regarding the development of lateral unsaturated flow. Moreover, there is a dearth of field data to substantiate its occurrence, and its importance to storm runoff is not well constrained.

In this study we undertook a collaborative field project designed to identify the hydrologic, weathering, and soil transport controls on shallow landslides and landscape evolution. The study site is a source area [after *Shreve*, 1969] to a channel head in the Oregon Coast Range, a region where shallow subsurface storm flow is the dominant runoff generation process and the soil profile remains largely unsaturated. Radiocarbon dating, landslide mapping, and numerical modeling have demonstrated that the hollow axes of steep, unchanneled valleys in this area periodically evacuate by shallow landslides that mobilize as debris flows [e.g., *Dietrich and Dunne*, 1978; *Reneau and Dietrich*, 1987; *Montgomery and Dietrich*, 1988; *Montgomery*, 1991; *Benda and Dunne*, 1997]. The objectives of this research were (1) to monitor the unsaturated zone response to steady irrigation to identify the unsaturated zone processes that determine the temporal and spatial characteristics of the pressure head response and (2) to determine how that unsaturated response affects pore pressure development and catchment discharge.

2. Location and Site Description

We conducted experiments in the Oregon Coast Range near Coos Bay, Oregon, where the annual rainfall is ~1500 mm [*Haagen*, 1989]. The study site is a logged but densely vegetated, small, steep, colluvium-mantled, unchanneled valley. The long and short hollow axes are about 41 and 18 m, respectively, and total area is ~860 m^2. Total relief between the channel head and the ridge top is ~43 m, average slope is 43°, maximum elevation is ~300 m, and slope aspect is due north (Figure 1). The site burned ~100 years ago, was clear cut in 1987, and was replanted with Douglas fir (*Pseudotsuga menzeisii*) seedlings in 1988. An application of herbicide (Roundup®) preceded replanting; present vegetative cover includes bramble (*Rubus*, i.e., salmon berry and thimble berry), sword fern (*Polystichum munitum*), and alder (*alnus*). Buried and partially buried logs up to 12 m long and 0.75 m in diameter were oriented toward the hollow axis. The only exposed bare soil occurred as mountain beaver (*Aplodontia*) burrow mounds. The burrows are typically part of a network [e.g., *Camp*, 1918; *Feldhamer and Rochelle*, 1982] and are up to 0.20 m in diameter.

Auger and core drilling data, examination of road cuts, and extrapolating information from three soil pits dug in a larger hollow ~70 m west of our site helped us determine soil and subsoil properties. Bedrock is Eocene turbidite sandstone of the Flournoy Formation [*Baldwin*, 1974], and it dips 8°–17° to the southwest, into the hillslope. The colluvial soil has a maximum vertical thickness of ~1.6 m at the hollow midpoint, thinning to zero on parts of the adjacent ridges. Fractured sandstone or saprolite underlie the colluvium. Well-developed saprolite occurs in the upper reaches of the site, but it is patchy and thinner downslope. Fractured sandstone outcrops locally along the topographic divide and just below the channel head, but we did not observe fresh bedrock or saprolite at the surface.

Haagen [1989] identified the soils as Haplumbrepts of the Bohannon series. Most of the colluvium mantle rests on weathered bedrock, and it has a large proportion of organic matter mixed with mineral soil because of intense biogenic churning. In three soil pits we found that slightly decomposed organic material, the O horizon, extends from the surface to ~0.10-m depth. The O horizon overlies a thick, granular, massive sandy loam along a clear but wavy contact of variable thickness. The B horizon is poorly developed at best or altogether absent. The C horizon is fractured and oxidized sandstone of variable thickness and is in smooth, abrupt contact with unweathered sandstone. *Anderson* [1995] reported that soil formation factors at our study site favor the development of Spodosols; however, recurring mechanical disturbances (e.g., tree throw, burrowing, and landsliding) preclude their formation.

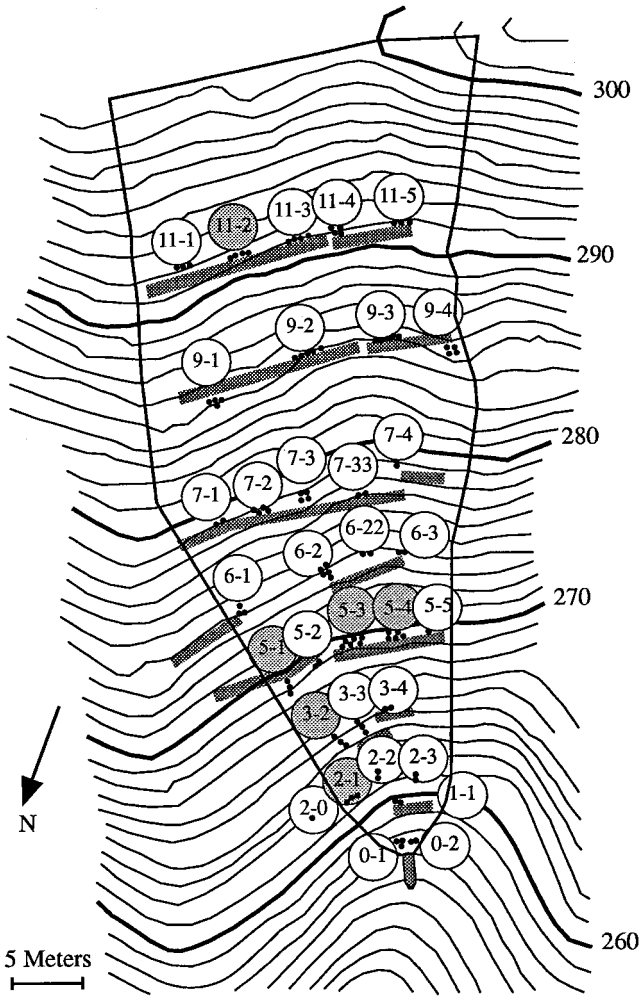

Figure 1. A 1-m contour map of the Coos Bay study site shows the relative position of tensiometers (dots), but the distances between them are not to scale. Tensiometer nests are identified by the encircled numbers; the shaded numbers represent the tensiometer nest locations where we determined in situ soil-water retention properties. The shaded rectangles across the site are access platforms, and a weir is shown at the base of the study site.

The upper 0.05–0.20 m of the A horizon has ~50% mineral soil and 50% live roots <1 mm in diameter. The remainder of the A horizon had ~10% gravel content by visual estimation of soil pit faces, with clast sizes ranging from 10 to 40 mm. The gravel occurred as slope parallel but discontinuous lines 1–3 clasts thick, or it was randomly distributed. Between 0.30-m depth and just above the underlying fractured bedrock the dry bulk density increased from 620 to 1200 kg/m^3. In one soil pit a single 10-mm diameter root extended to the C horizon.

This low-density, gravelly, sandy loam is so highly permeable that saturated hydraulic conductivity determination with the Guelph Permeameter [*Reynolds and Elrick*, 1985] was not possible because we could not maintain a constant head of water. However, *Montgomery et al*. [1997] measured in situ saturated hydraulic conductivity by the falling head method, and they showed that the saturated hydraulic conductivities across the study site were variable but ~10^{-3} m/s in the colluvial soil and 10^{-5} m/s in the saprolite. Recurring mechanical disturbance and a high soil organic content combined with the potential for preferential flow along roots, root casts, partially buried logs, and burrows create conditions that favor a high saturated permeability. Soil-water retention properties (see below for methodology), however, indicate that while the soil may permit the rapid transmittal of saturated throughflow, it has low water retention relative to total porosity.

3. Experimental Design and Methods

We determined in situ soil-water retention properties at six locations (Figure 1) by simultaneously monitoring the soil-water content and pressure head response to plot irrigation. The plots were <0.5 m^2, and they were centered around previously established tensiometer nests. The plot locations represent the ground cover of our study site: a sparsely vegetated mineral soil, a densely vegetated mineral soil, and the O horizon. Prior to irrigation we clipped the plot vegetation, but left the O horizon intact. Irrigation rates varied between 370 and 5725 mm/h, and durations varied from 0.18 to 0.50 hours (Table 1). The unusually high irrigation rates were needed to create a wide range of soil-water contents. We monitored soil-water content with 0.30- or 0.45-m-long wave guides connected to a TRASE® time domain reflectometry system [*Skaling*, 1992]. The vertical wave guides had their tops coincident with the top of the mineral soil and at least 0.2 m from the nearest tensiometer. We monitored the pressure head and soil-water contents at 1-min intervals for a 10-min period before irrigation and up to steady state, and at 1- to 2-min intervals for the 0.1- to 0.4-hour steady state period. In two cases (nests 2-1 and 3-2) we step increased the applied flux during steady state to increase the steady soil-water content. The drainage response was monitored at 0.5-min intervals initially and at variable intervals later for up to 1.5 hours; at least one additional measurement was made over the following 24 hours. We then used the transient response data to construct soil-water retention curves.

Montgomery et al. [1997] describe the piezometer, weir, rain

Table 1. Small Plot Irrigation and Site Characteristics

Site Number	Surface Type	Plot Size, m^2	Intensity, mm/h	Duration, hours	Ponding Time, hours
2-1	densely vegetated	0.17	1450	0.18	0.10
			370	0.50	0.04
3-2	O horizon	0.21	1960	0.10	
			5720	0.20	
5-1	densely vegetated	0.31	940	0.30	0.04
5-3	sparsely vegetated	no data	no data	0.22	no data
5-4	O horizon	no data	no data	0.28	no data
11-2	sparsely vegetated	0.26	3800	0.37	0.17

gauge, sprinkler installation and data acquisition, and the site infrastructure. At the catchment scale we used 13 sprinklers to simulate nonponding precipitation events of 1.5 ± 0.8 and 3.0 ± 0.9 mm/h of ~6 and 4 days duration (experiments 1 and 2, respectively). Moreover, on the final day of experiment 2 a natural storm augmented the applied rain between about 2:00 A.M. and 7:00 A.M. PST, and between 5:00 A.M. and 5:10 A.M. PST the total rain intensity increased nearly 10-fold. Also, just prior to sprinkler shut down for experiment 1, we acquired soil samples from the valley axis along row 8 with a piston core device (78-mm ID) to characterize the steady state soil-water content-depth profile.

We monitored the unsaturated zone pressure head response with 19 standard and 81 high-flow ceramic cup tensiometers distributed across the study site to 33 locations along eight rows (Figure 1). Each location had one to six tensiometers installed at roughly 0.25-m-depth intervals, and in each nest, individual tensiometers were spaced 0.1–0.3 m apart, along contour when possible. The distance between nested groups of tensiometers was 1.5–5.0 m in the cross slope direction and 3.0–10.0 m apart in the downslope direction. At the ground surface a bentonite cap around the tensiometer barrel prevented water from flowing along it.

Four hand-held, digital readout pressure transducers (Tensimeter® [see *Marthaler et al*., 1983]) were used to read all tensiometers. We found that the pressure transducer calibrations were accurate to 1 mbar over the range of pressures observed in the field, and we determined the tensiometer system response times [e.g., *Cassel and Klute*, 1986] were about 5 s. In the field we monitored the pressure transducers for drift by reading a "standard" tensiometer before, during, and after each set of tensiometer readings. The standard was a known pressure head tensiometer standing in a sealed water column. Time series of standard readings show that diurnal temperature effects and instrument drift on pressure readings were negligible. It took ~40 min to read all tensiometers, and during each experiment the number of readings varied depending on the transient nature of the pressure head response and physical limitations. During daylight hours of experiment 1, data were initially gathered at 2-hour intervals for 10 hours and up to 6-hour intervals thereafter. At night, during both experiments, we usually made two instrument readings. During experiment 2 the interval was shortened during transient conditions and lengthened during approximate steady state.

To compare the temporal attributes of the discharge response with the temporal and spatial attributes of the saturated and unsaturated pressure head response, we developed a procedure to identify the approximate time to steady state response on the basis of exponential decay. *Horton* [1940] used a similar approach to determine time to steady state infiltration rate. We chose this simple empirical relationship because it fits the data well and it requires only one parameter, T, to determine a best fit line. The equation used to identify approximate time to steady state is

$$\psi(t) = \psi_f - (\psi_f - \psi_i)\ \exp\left(-\frac{t}{T}\right), \qquad (1)$$

where $\psi(t)$ is the pressure head or discharge time series, ψ_f is the final pressure head or discharge over the time interval of interest, ψ_i is the initial pressure head or discharge over the time interval, and t is the independent variable time since the start of the interval of interest. T is the time required to produce 63% (e^{-1}) of the full response ($\psi_f - \psi_i$). We estimated the approximate time to steady state as $3T$, the time to reach 95% of the full response. Equation (1) was applied separately to rising and falling periods of the data. The rising period begins at the start of irrigation, and the drainage period starts at the end of irrigation.

In the curve-fitting procedure, one enters a value for T, and it is automatically adjusted in an iterative process to improve the best fit line on the basis of least squares regression, a standard feature in Kaleidagraph®. Data with a time to first response that exceeded 12 hours had the curve fit applied to it without the lag, and the resulting approximate time to steady state was $3T$ plus the lag time. This modification applied to nearly all piezometers and a total of seven tensiometers. Under draining conditions, (1) generally was applicable. In some cases, however, piezometers became dry before the calculated approximate time to steady state, and times to zero pressure head approximated time to steady state. For brevity, hereafter we will refer to approximate steady state as steady state.

During these irrigation experiments, only the unsaturated zone in the soil mantle was monitored, but the unsaturated zone must have extended into the underlying fractured bedrock, at least during initial wetting. Hence the effects of unsaturated fracture flow on storm runoff and pore pressure development were not monitored.

4. Results

4.1. Soil-Water Retention and Hydraulic Conductivity Curves

Plot irrigations (Table 1) produced incipient ponding, but no surface runoff occurred, and most tensiometers responded to irrigation within 2.5 min. Most time series developed an eventual steady state response, and after irrigation the pressure heads declined at a rate much lower than during the rise. At nest 2-1, large positive pore pressures were detected at 0.27 m (Figure 2a); slight positive values occurred at 0.70 m, but at 0.53 m, pressure heads remained negative. Nest 3-2 also had positive pore pressure at 0.41 m (Figure 2b), and nest 5-4 shows that the tensiometer response at 0.77-m depth preceded the 0.52-m response (Figure 2d). At nests 3-2 and 5-3 we step increased the applied flux, and there was a large positive pressure response in 3-2, but none in 5-3 (Figures 2b and 2c).

The soil-water retention curves have a number of similarities (Figure 3). For example, after soil-water contents increased by ~0.10 m^3/m^3 from their initial values, pressure heads were at or near-zero. In the near-zero range the wetting curves steepened considerably, and the soil-water content became highly variable. Conversely, distinct differences between the retention curves occurred. For example, the minimum soil-water content at which the wetting curve steepens is variable; the drainage curves have variable slopes; five curves show hysteresis (Figures 3a–3e); two curves illustrate a break in slope on the draining curve (Figures 3c and 3d), indicating that further displacement of soil-water by soil-air may not occur until ~0.20 m of suction is applied. For all irrigations the highest volumetric soil-water content attained was 0.60 m^3/m^3, a value approximately equal to saturation. The air entry pressure for a completely saturated soil sample was indeterminate with our experimental design.

We estimated the unsaturated hydraulic conductivity function with the *van Genuchten* [1980] method, parameterized for a sandy loam [*Carsel and Parrish*, 1988]. Overall, the characteristic curve mimics the soil-water retention curves, having a highly variable unsaturated hydraulic conductivity as pressure

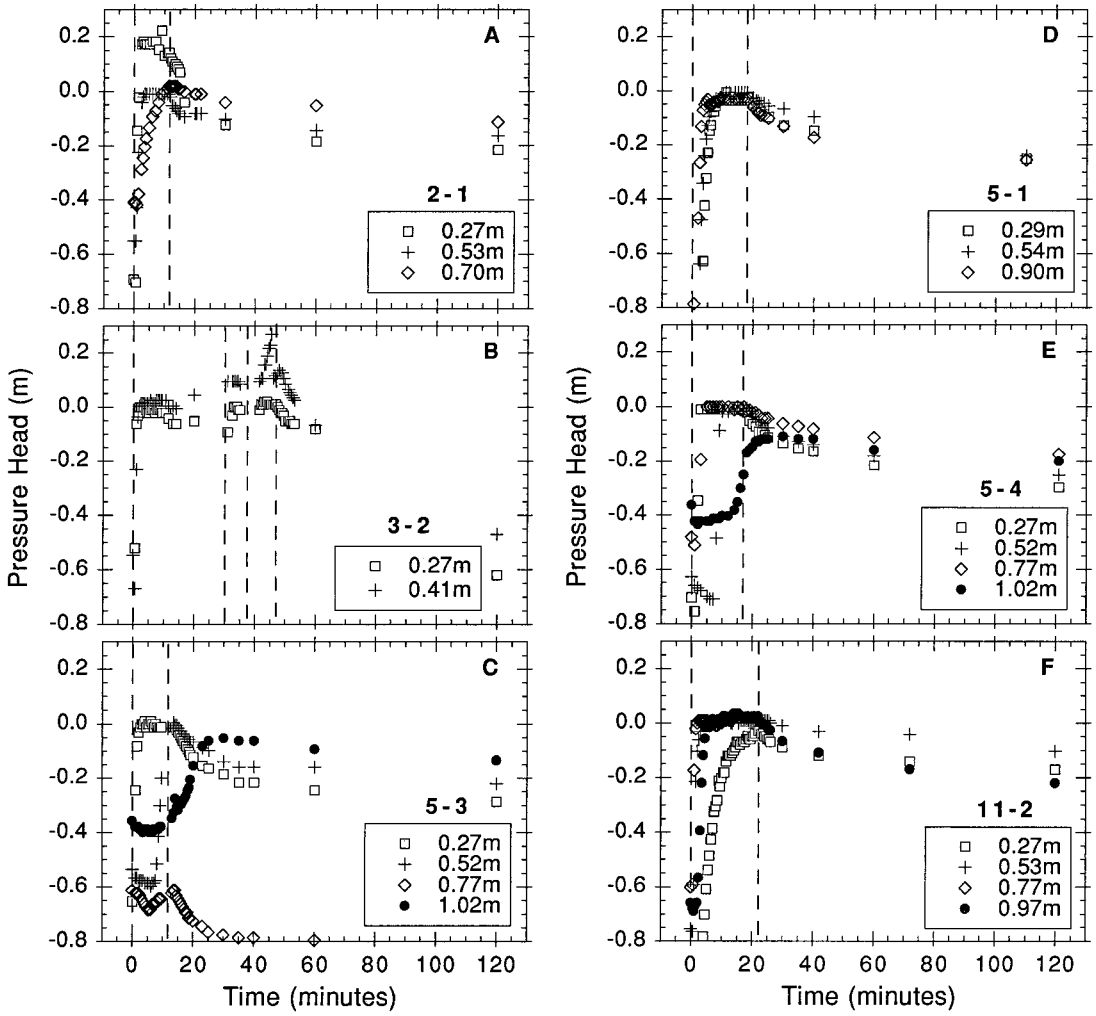

Figure 2. Pressure head time series of the plot irrigation experiments summarized in Table 1. The dashed vertical lines correspond to irrigation intervals. Figures 2b and 2c show the response to step increases in applied water flux. In Figure 2c, however, the flux changes were not recorded.

heads approach zero (Figure 4). For example, at pressure heads between −1.00 and 0.00 m the unsaturated hydraulic conductivity varies over seven orders of magnitude. At −0.25-m pressure head the unsaturated hydraulic conductivity is of the same order of magnitude as our irrigation rates (10^{-7} m/s), but between pressure heads of −0.25 and 0.00 m the predicted unsaturated hydraulic conductivity was higher than the irrigation rates.

4.2. Pressure Head and Total Head Time Series

The applied rain produced a distinct pressure head increase, and with continued irrigation most of the soil profile developed near-zero pressure heads, and some pressure head time series showed distinct diurnal variations. At the end of irrigation, pressure heads declined exponentially before attaining a new steady state value. Histograms of pressure heads taken just prior to irrigation, during quasi steady state, and after two days of drainage summarize the dynamic response of the unsaturated zone. Pressure head distribution differences between experiments 1 and 2 (Figure 5) reflect the much wetter initial condition for experiment 2 than for experiment 1, and at steady state, more pressure heads were closer to 0.0 m for experiment 2 than for experiment 1 (Figures 5b and 5e). After 2 days of drainage, however, the pressure head distributions were similar (Figures 5c and 5f). Table 2 depicts the summary statistics for histograms.

Most tensiometers between 0.16- and 1.03-m depth showed diurnal variations of ~0.02–0.06 m with diurnal maxima between midnight and 0400 hours, and minima at midafternoon to late afternoon. Time series of the tensiometer standard (see section 3) do not reveal any systematic variations in pressure head; hence the diurnal pressure head variations are not an artifact of instrumentation. Instead, the diurnal signal was driven by daily variations in evapotranspiration and winds which reduced the amount of applied water through increased evaporation and transport of water droplets offsite.

The diurnal oscillations in pressure head translate to diurnal oscillations in total head (Figures 6b–6f), and in some cases the oscillations show a progressive delay with depth. During experiment 1, for example, tensiometers in nest 9-4 had daily maxima that occurred 2–4 hours earlier at 0.26 m below the surface than at 1.00 m (Figure 6f). The propagation rate of depth-varying diurnal oscillations suggests that head variations can pass relatively quickly through the unsaturated soil.

We combined tensiometer and piezometer data to establish total head fields so that we could infer flow paths in downslope

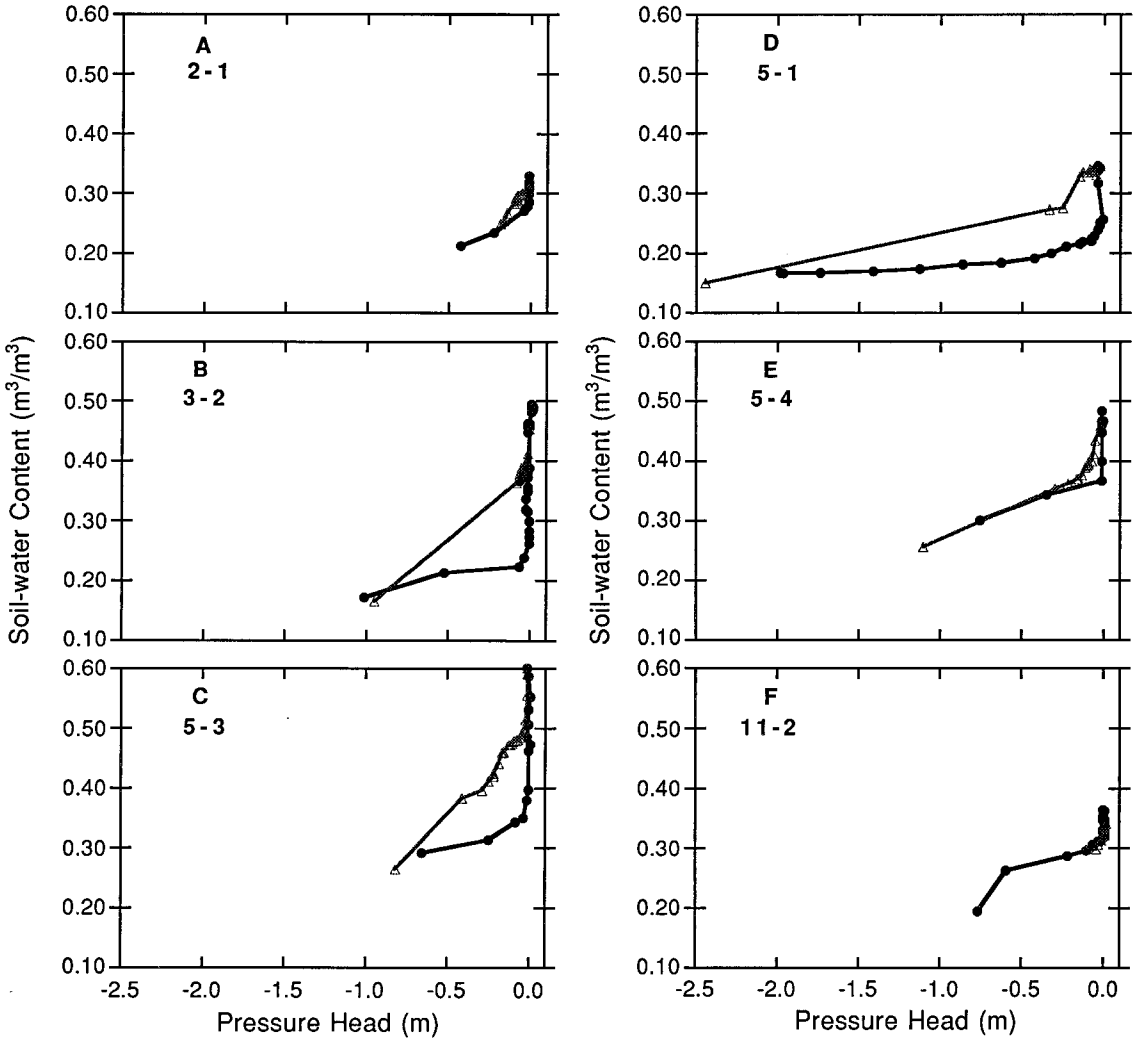

Figure 3. In situ soil-water retention curve data. The identification numbers correspond to the shaded locations of Figure 1. The wetting curves are black dots, and the drainage curves have open triangles. Experiments at nest 2-1 experienced instrument failure.

and cross slope transects, and in all cases we assumed that flow paths were orthogonal to total head lines. We did not detect a downslope unsaturated flow component. In these total head calculations, however, the elevation head gradient was much greater than the pressure head gradient [e.g., *Anderson and Burt*, 1978], and under these conditions, vertically downward flow paths should prevail. We speculate, however, that a closer tensiometer spacing may reveal a downslope unsaturated flow component.

The thick soil accumulation and the dense tensiometer and piezometer coverage make row 5 the best transect to represent cross-slope equipotential fields and to infer unsaturated flow paths. Experiments 1 and 2 had initial cross-slope components of 0.34 and 0.20, respectively, directed toward the hollow axis (Figure 7a). After 8 hours of irrigation the lateral components diminished (Figure 7b), and after ~24 hours the lateral component became negligible and flow paths were nearly vertical. The vertical flow paths seem not to be affected by the underlying boundaries, and flow paths pass unperturbed through the soil and into the saprolite or fractured bedrock (Figure 7c). After 99 hours a water table developed, but the unsaturated flow paths seem unaffected (Figure 7d).

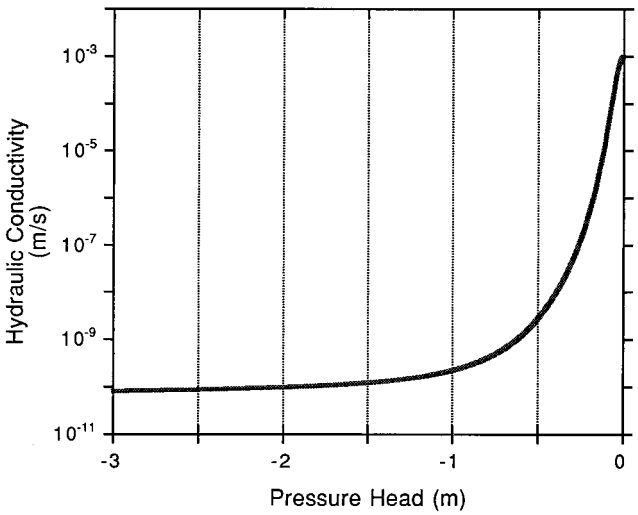

Figure 4. The unsaturated hydraulic conductivity function as determined by the method of *van Genuchten* [1980] using the sandy loam parameters of *Carsel and Parrish* [1988], $\alpha = 0.075$ and $N = 1.89$.

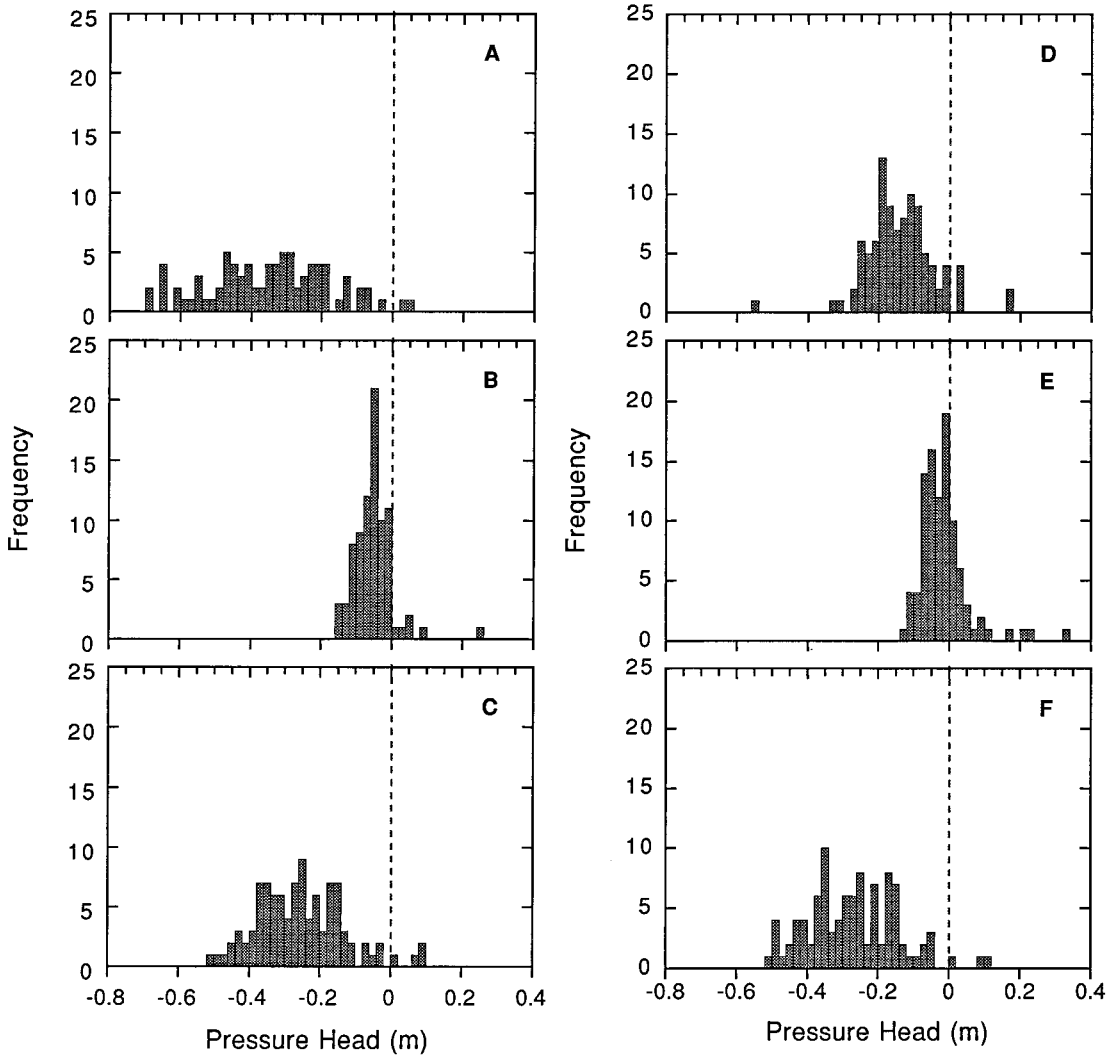

Figure 5. Summary histograms for experiments 1 and 2 detailing the pressure head distributions (Figures 5a and 5d) just prior to the start of irrigation, (Figures 5b and 5e) at the start of steady discharge, and (Figures 5c and 5f) two days after the irrigations ended. The dashed vertical line in each plot identifies zero. Bin size equals 0.02 m. Figures 5a–5c correspond to experiment 1, and Figures 5d–5f correspond to experiment 2.

Time series of the row 5 total head fields also show that a head gradient front, identified as a 0.3–0.6 m/m change in gradient, advanced through the soil profile at a decreasing rate (Figures 7a–7d). For example, the head gradient front advanced at 0.07 m/h, but after ~8 hours the rate decreased to 0.05 m/h, and after 24 hours the rate decreased to 0.03 m/h. The decreasing rate may arise from a decrease in capillary forces that augment water percolation into a soil profile or from vertical heterogeneity due to increased bulk density with depth.

4.3. Time to First Response and Time to Steady State

Horton and Hawkins [1965] showed that soil-water can advance through a soil profile by a displacement process. Consequently, the wetting front and the position of newly applied water may not coincide. For 1-D, gravity-dominated flow, with a constant soil-water content at the ground surface, *Stephens* [1996] approximated the wetting front velocity V_{wf} and infiltrating water velocity V_w as

Table 2. Summary Statistics for Histograms

Experiment	Duration, hours	Irrigation Rate, mm/h	Number of Tensiometers Used	Mean Initial Pressure Head, m	Mean Steady Pressure Head, m	Mean Postirrigation Pressure Head, m
1	142	1.5 ± 0.8	81	−0.35 ± 0.17	−0.05 ± 0.05	−0.25 ± 0.12
2	96	3.0 ± 0.9	100	−0.14 ± 0.09	−0.01 ± 0.07	−0.27 ± 0.13

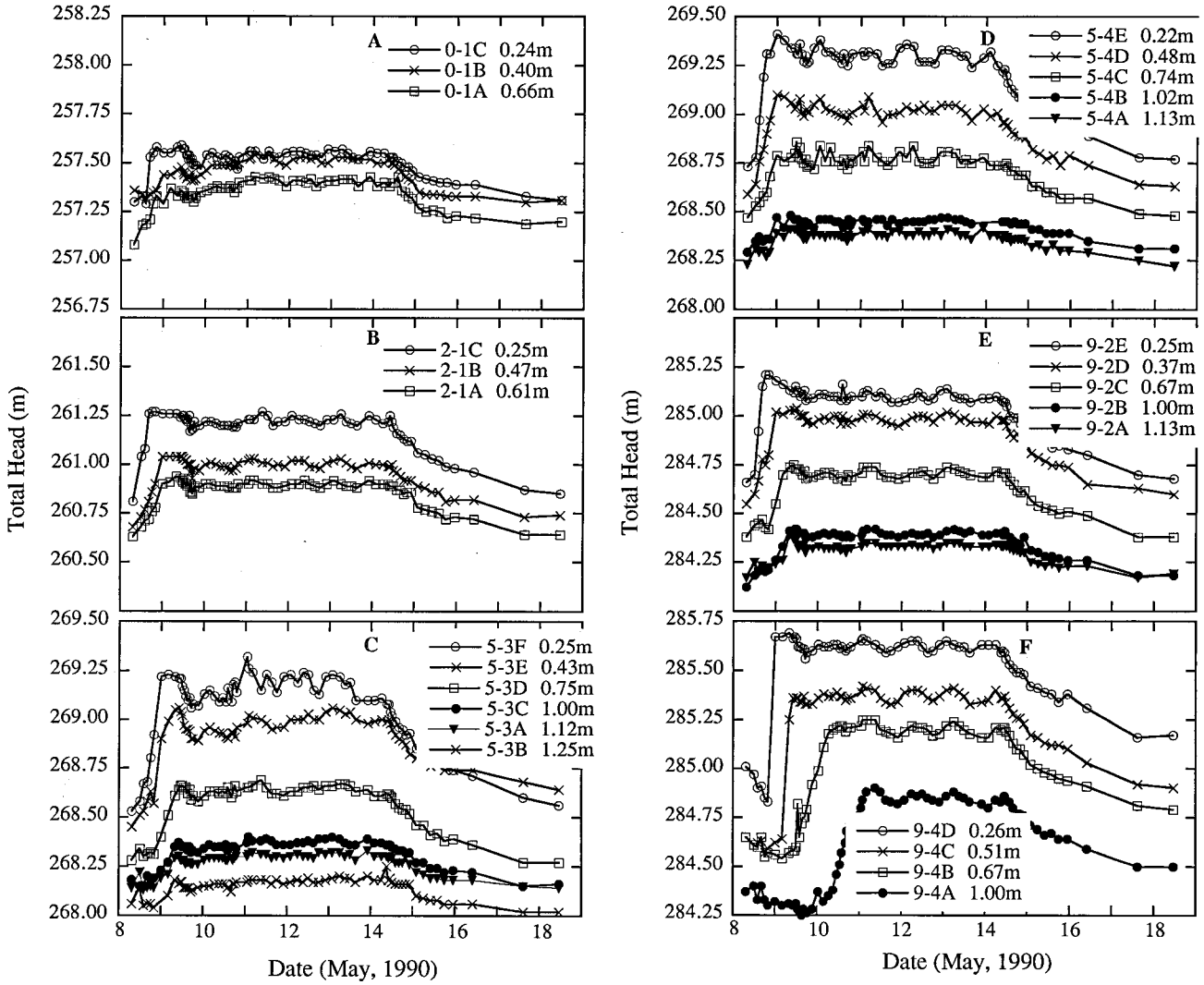

Figure 6. Representative time series of total head during experiment 1. The identification numbers on each time series refer to the tensiometer nest identification numbers of Figure 1, and the following number is the tensiometer depth in meters. The first reading in these time series corresponds to the pressure heads just prior to the experiment 1 sprinkler tests, and the second reading represents the actual start of experiment 1.

$$V_{wf} \approx \frac{K(\theta_0)}{\theta_0 - \theta_i} \tag{2}$$

$$V_w \approx \frac{K(\theta_0)}{\theta_0}, \tag{3}$$

where K is the unsaturated hydraulic conductivity, θ_0 is the soil-water content behind the wetting front, and θ_i is the initial soil-water content. In the case of our two nonponding irrigation experiments the unsaturated hydraulic conductivity behind the wetting front was equal to the irrigation rates, and $\theta_0 = 0.45$ and $\theta_i = 0.15$; these values produced maxima for $V_{wf} = 0.010$ and $V_w = 0.007$ m/h. We used these approximations to determine if the pressure head response in the soil profile was fast or slow.

"Wetting front" arrival time was estimated as the first time of three consecutively increasing tensiometer pressure head values. Arrival times ranged from 2 to 38 hours for experiment 1 and from 3 to 17 hours for experiment 2. Tensiometer depth divided by arrival time indicates that at the onset of irrigation a pressure head signal advanced through the soil profile an average of 15 times greater than the estimated water and wetting front velocities. Hence initial pressure head response appears to be driven by the passage of a pressure wave rather than the advective arrival of new water.

We approximated time to steady state in each tensiometer response with (1), and we examined the spatial pattern of time to steady state for experiments 1 and 2. Average time to steady state during wetting was 31.1 ± 21.7 hours for experiment 1 and 18.5 ± 10.4 hours for experiment 2. There was no discernible pattern of time to steady state as a function of position in the catchment, despite large differences in initial soil-water content as inferred by initial pressure heads. Time to steady state as a function of soil depth, however, (Figure 8) reveals a clear depth dependence for the wetter initial conditions of experiment 2 (Figure 8). In both experiments, time to steady state increased by ~1 hour per 0.02–0.03 m of flow distance. This speed is ~2–4 times faster than that for the wetting front and infiltrating water.

Once irrigation ended, the unsaturated zone drained and pore pressures fell and approached a slowly changing, quasi steady state in 80.8 ± 28.5 hours for experiment 1 and in 49.6 ± 12.4 hours for experiment 2. In both cases, time to steady state was independent of soil depth. It seems that as soil-water contents dropped sufficiently and pressure heads decreased, spatial heterogeneity in soil-water retention properties produced significant variability in the spatial distribution of pressure heads. This observation supports the prediction of *Yeh et al*. [1985].

Some of the variability in response shown in Figure 8 for the wetting condition may be due to effects of local variability in irrigation rates. Local irrigation rates differed across the catchment by a factor of ~9, but at the tensiometer nests, irrigation rate varied by a factor of 4. We examined the effects of local irrigation rates on the time to steady state and time to first response. We found that times to steady state and times to first response were not correlated with irrigation rate. This finding is compatible with theoretical predictions showing that high-frequency effects of temporally variable irrigation will be damped with increased depth [*Gardner*, 1964].

In order to compare the discharge response with the unsaturated and saturated responses we constructed a graph in which the time to steady state for wetting was plotted relative to that for draining periods of tensiometers, piezometers, and weir data. By plotting the time to steady state for the discharge rising limb as a vertical line, and that for the recession limb time as a horizontal line, we created distinct quadrants of response types. We then plotted the wetting and draining times to steady state for the tensiometer and piezometer data on the same graph (Figure 9). Nearly all of the tensiometer data for experiments 1 and 2 fell in the quadrant in which the time to steady state was less than that for the discharge on the rising limb and more than that on the falling limb. No distinction existed between those tensiometers that showed only unsaturated response and those that indicated slight positive pressures.

Upon cessation of the applied rainfall the saturated zone rapidly declined, and all the piezometers drained before the discharge approached steady base flow and well before the tensiometers reached steady state. In experiment 2, although the wetting time to steady state in the piezometric response was longer than most tensiometers but less than the discharge time to steady state (as in experiment 1), under draining conditions some of the piezometers continued to respond after the falling limb of the hydrograph reached steady state (for other observations documenting delayed piezometric response to rainfall, see *Montgomery et al*. [1997]). Piezometric times to steady state for experiment 2 show that for individual piezometers the longer the time to steady state on the rising limb, the longer this time on the falling limb; this pattern was not recorded in the tensiometer data of either experiment (Figure 9).

Overall, our field site reveals a simple result regarding the evolution of a steady state soil profile. After irrigation began, rapidly advancing pressure head changes caused steady state to develop first in the unsaturated zone, next in the saturated zone, and only after the saturated response was complete did the discharge reach steady state. During the steady state period of both experiments 1 and 2 the soil profile remained largely unsaturated (Figure 10). At the end of irrigation the time to steady state in piezometers may precede or follow the discharge time. In either case the decline in discharge and saturated response must have resulted from a declining unsaturated flux. The perched water table surface fell below our piezometers, and the discharge approached a near steady base flow well before the unsaturated zone drained toward steady pressure heads. The steepness of the site favors rapid drainage of the saturated zone when flux to it from the overlying unsaturated zone decreases, and the unsaturated zone is the last to reach steady state. Of course, these three distinct elements are interdependent and begin to respond at roughly the same time; it is the time to full response that distinguishes their behavior.

4.4. Spike Increase in Rainfall and the Rapid Discharge Response

The applied irrigation rate ($\approx 10^{-7}$ m/s) for both experiments was about 4 orders of magnitude less than the saturated hydraulic conductivity ($\approx 10^{-3}$ m/s) of the soil at any depth. Although the application rate was low, the duration was 6 and 4 days. By the time the cumulative irrigation was ~50 mm, most of the unsaturated zone was driven to near-zero pressure head. With the soil profile in the near-zero range a strong temporal linkage between the unsaturated zone, saturated zone, and discharge occurred. The linkage was exemplified by the catchment's hydrologic response to a high-intensity burst of natural precipitation that fell during the latter part of experiment 2.

At 2:00 A.M. PST on the final day of experiment 2 a natural storm augmented the applied rain, and from 5:00 to 5:10 A.M. the total rain intensity increased 10-fold. At 7:00 A.M. the natural storm ended and at 9:30 A.M. the sprinklers were shut off. Despite this 5.5-hour period of increased rainfall intensity, no changes beyond the noise in the pressure head readings in the unsaturated zone occurred. Tensiometers were not monitored during the 5:00 A.M. spike of rainfall, but tensiometer measurements at 7:00 A.M. show no response to this storm event. The peak rainfall to peak response in recording piezometers and discharge, however, showed lags of 1.7 and 2.5 hours, respectively. We interpret these observations to indicate that a spike of rainfall upon a near-zero pressure head field produced a pressure wave that advanced through the unsaturated soil profile much faster than the newly applied water, and as the pressure wave advanced it caused the rapid effusion of old, stored soil-water.

5. Discussion

5.1. Boundary Effects

The lower boundary to unsaturated flow through the soil varied as (1) a transition to saturated flow, (2) a transition to unsaturated saprolite, or (3) a transition to unsaturated weathered bedrock. This lower boundary had a strong cross-stream slope to it (Figure 7); hence if transitions 2 or 3 represented significant barriers to flow, then water would tend to pond at the transition, and not only would saturated lateral flow occur, but so should lateral unsaturated flow. We found no evidence for head gradient deflections at any of these three boundaries and detected only minor components of cross-slope head gradients during dry periods. There are at least two reasons for this lack of material and topographic effect on the unsaturated flow field. First, the soil-water retention curve is very steep in the near-zero pressure head range, so only minor changes in head are needed to match the unsaturated zone pressure head with that in the saturated response areas. Second, the irrigation rates were modest and caused delivery of water through the soil profile that did not exceed the conductivity of the saprolite

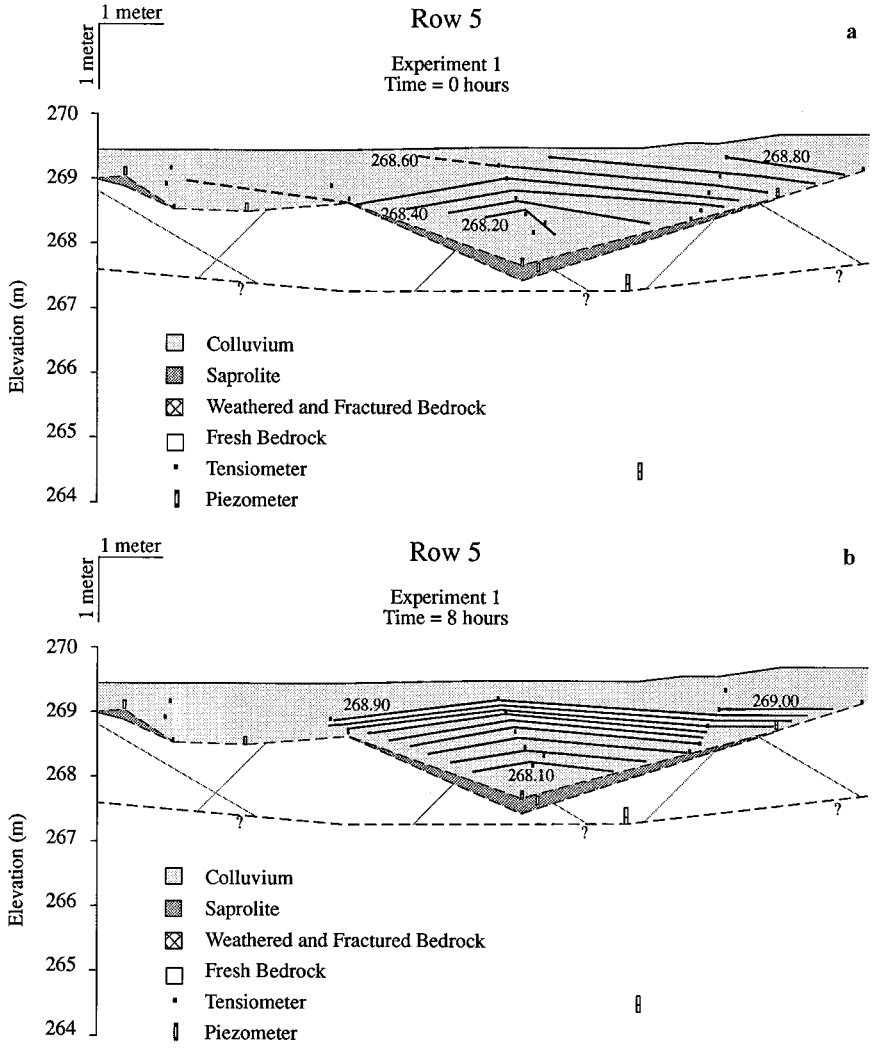

Figure 7. Total head contour plots along a section through row 5 at (a) 0, (b) 8, (c) 24, and (d) 99 hours into experiment 1. All views are looking upslope and are centered on the region with instrumentation; the contour interval is 0.10 m and is dashed where inferred.

or weathered rock; hence there was no head gradient change associated with water entering these materials from the soil. It is possible that more intense rainfall and thus vertical flow rate would lead to ponding at these material boundaries, but then, again, because of the soil-water retention properties, we anticipate the deflection of flow lines to be minor. Under relatively wet conditions, therefore, cross-slope and downslope unsaturated flow seems unlikely at our site.

The initial cross-slope, unsaturated flow component resulted from the lowest-pressure heads (and driest soils) being in the upper reaches of the soil profile, along the hollow axis. This condition may prevail in thicker soils where the evapotranspiration-affected upper soil profile is farthest from the wetter subsoil. Nonetheless, the result was that equipotential lines were pulled upward, leading to a net lateral transport toward the hollow axis. This finding was contrary to our initial expectation that the lateral flow component resulted from topographically induced convergence. With continued irrigation, however, the lateral component diminished, and flow paths became essentially vertical through the soil profile.

Anisotropy in the colluvium mantle may cause flow paths to follow trajectories that are not orthogonal to equipotential fields. Although we did not attempt to quantify anisotropy, we speculate that during the approximate steady state period the near-zero pressure head field produced a negligible head gradient in the principal directions of anisotropy; hence vertical downward flow paths should prevail. It is unlikely that steady state flow paths were anything other than orthogonal to equipotential fields.

The apparent one-to-one correspondence of piezometer time to steady state wetting to that of draining (Figure 9) is predicted from simple hydrologic models such as that by *Iida* [1984], in which the bedrock is assumed to be impermeable. In his model for both the wetting and draining conditions, steady state is reached first at the top of a hill and spreads downslope until the entire catchment is in steady state. However, at our site the deepest piezometers were in the upper part of the catchment, and they responded the most slowly; therefore our data do not support Iida's prediction. Instead, the pattern may have resulted from both a depth dependency and local variations in saturated conductivity, with piezometers in lower-conductivity sites having longer times to steady state. Absence

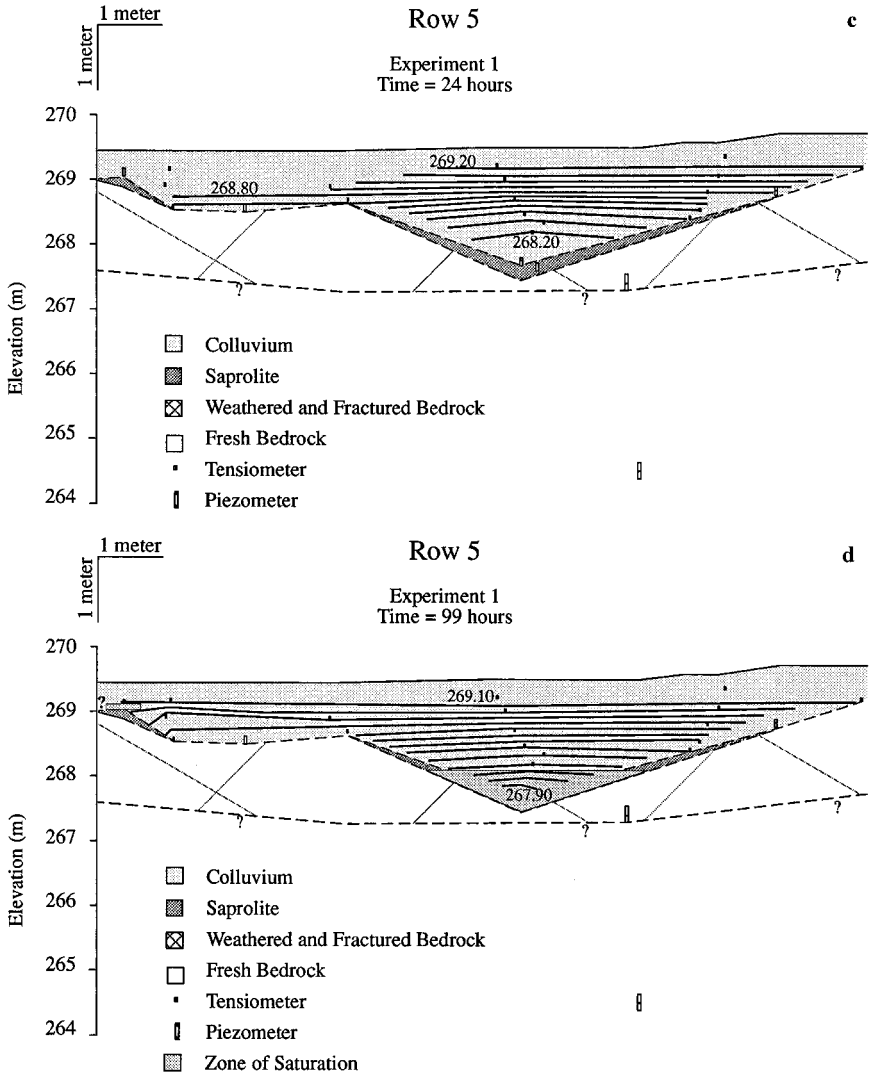

Figure 7. (continued)

of a similar response pattern in the tensiometer data presumably resulted from the difference in boundary conditions and drainage properties. With the onset of rainfall the soil wets from the surface and drains freely at the bottom; hence the deepest tensiometer should respond last. At the end of irrigation, drainage at the base and a lack of resupply at the surface coupled with hysteretic effects may preclude a spatial structure in time to steady state.

5.2. Preferential Flow

Two observations suggest that preferential flow may occur at our site. First, the high-intensity plot irrigation experiments used to develop the soil-water retention curves revealed a rapid deep response to water application (Figure 2). These deep (1 m or more), rapid (a few minutes) responses may result from preferential flow along macropores [e.g., *De Vries and Chow*, 1978] or saturated mesopores [e.g., *Wilson et al.*, 1990]. The high irrigation rates, however, may have caused air encapsulation in the vicinity of the tensiometer cup, giving rise to rapid response characteristics and higher pressure heads. In either case the irrigation rates that led to this response were extremely high and far in excess of any natural rainfall intensity. These intensities were necessary, however, to document the full range of the soil-water retention curve when starting with a fairly dry soil.

The second observation that may indicate preferential flow is the short time to first response in the deep tensiometers during experiments 1 and 2. This response may also result from air entrapment or the rapid passage of a pressure wave in response to water loading rather than rapid vertical advection.

Although during the wetting up period there may be some preferential flow, several observations suggest that it is not important during storm events. *Anderson et al.* [1997a, b] have shown that nearly all runoff is old water. In addition, they have shown that the new water runoff component comes primarily from just upslope of the channel head, at the weir, and that during wet conditions the water travels through the soil as plug flow. Unlike other sites where preferential flow has been stressed [e.g., *Mosely*, 1979], the soil mantle of our study site is a sandy loam, free of significant pedogenic structures that may favor preferential flow. Large burrows and root holes do exist, but these only become significant avenues for bypassing the unsaturated zone if rainfall intensities are extraordinarily high or if flow is locally concentrated by such things as fallen logs.

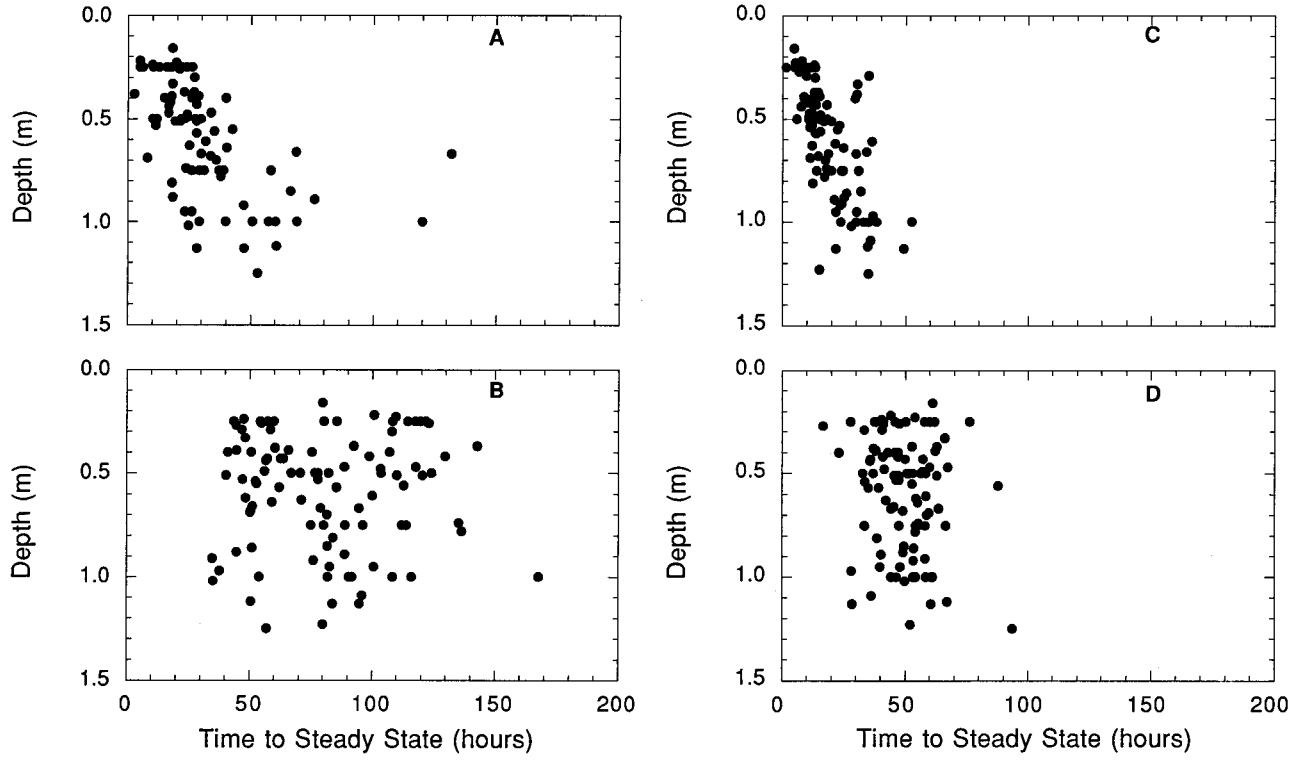

Figure 8. Tensiometer wetting and draining times to steady state plotted against depth for experiments (a) and (b) 1 and (c) and (d) 2.

Hence, while our experiments do not preclude preferential flow as a significant contributor to runoff, available evidence suggests that it may only be important during initial wetting or during very intense storms.

5.3. Soil-Water Retention Properties and Macropores

The micropore, mesopore, and macropore size and function model proposed by *Luxmoore* [1981] and *Luxmoore et al.* [1990] provides a useful conceptual framework for relating the unsaturated zone response to our catchment hydrologic response, and it connotes a dependence of the hydrologic response on the temporal development of unsaturated zone processes and subsurface flow paths (e.g., connect-disconnect hypothesis [*Luxmoore and Ferrand*, 1993]). Here pressure heads greater than −0.05 m correspond to Luxmoore's macroporosity, and from the plot irrigation response characteristics we reason that in the near-zero pressure head range, soil-water contents greater than ~0.35 m^3/m^3 will persist only as long as there is an applied flux across the ground surface. Indeed, when we step increased the applied flux at two selected subplots, the new steady state soil-water content was 0.07–0.10 m^3/m^3 higher, but we did not always detect a clear pressure head response. These observations suggest that a spike increase in rain intensity upon a near-zero pressure head field may register a negligible pressure head response.

Assuming that the −0.05- to 0.00-m pressure head range corresponds to equivalent macroporosity, we can approximate the total volume of macropores as the difference between a fully saturated soil sample, ~0.60 m^3/m^3, and a "drained" soil sample, about 0.30 m^3/m^3. Hence about one half of the pore space, or ~0.30 m^3/m^3 of the bulk soil volume, consists of noncapillary macropores; the presence of mountain beaver burrows makes the 0.30-m^3/m^3 value a minimum estimate, although we could not determine if these were hydraulically active. Overall, the soil is difficult to saturate, and soil-water drains readily at higher soil-water contents associated with near-zero pressure heads. Moreover, tension saturation in the presence of a perched water table is unlikely because of the abundance of noncapillary-sized pores. We also infer that the soil mantle and the steep hillslope angle should favor the dissipation of perched saturated zones. *Montgomery et al.* [1997] observed thin and discontinuous zones of saturation for experiments 1 and 2, however, and they reasoned that a regular exchange of saturated throughflow between the underlying fractured rock and the colluvial fill occurred.

5.4. Pressure Waves

Soils with hydraulic properties that yield steep soil-water retention and characteristic curves in the near-zero pressure head range (Figures 3 and 7) may favor the development of pressure waves. When such a soil is in the near-zero range, a rain spike may produce a slight increase in pressure head and a corresponding large increase in conductivity. The increased conductivity and the slight increase in head gradient produce a rapid release of old water as the wave propagates downward. Moreover, the near-zero pressure heads dictate that a near-unit head gradient prevail; hence the unsaturated hydraulic conductivity assumes most of the burden in accommodating increased flux.

The concept of pressure waves advancing through a soil profile is not a new one. For example, *Smith* [1977] identified the conditions necessary for evaluating soil-water movement as a shock wave. Smith found that when the soil-water content profile is nearly uniform, changes in flux translate directly into

changes in soil-water content that rapidly advance through the soil profile. Also, *Marui et al*. [1993] observed spiked and damped discharge responses to rainfall during the wet and dry seasons, respectively. They went on to speculate that pressure wave transmission occurred through a continuous water phase or through entrapped air. Our observations substantiate the predictions of Smith, and they highlight an important soil property for pressure wave development: highly variable soil-water contents in the near-zero pressure head range.

5.5. Slope Stability

In November 1996 our study site failed as a shallow landslide below row 7. Although we did not have recording tensiometers at the site, the results reported here provide some insight about the role of unsaturated flow on slope stability. *Montgomery* [1991] and *Montgomery et al*. [1997] showed that other slope failures in the vicinity were associated with short pulses of high-intensity rain in the midst of a storm that led to exfiltration head gradients from bedrock into soil. For this to happen the pulse of rain must be transmitted relatively quickly through the unsaturated zone, much more quickly than by advection. Such a condition exists at our study site when the soil-water content is high and the pressure head field is near-zero. The rapid displacement of preexisting soil-water into the saturated zone can generate a rapid pore pressure rise. Hence, once the soil is wet, pulses of rain can lead to rapid pore pressure rise in the saturated zone and to slope instability. Our field data also support *Humphrey*'s [1983] contention that estimates of response time for pore pressure rise and discharge must include the time lag due to travel through the unsaturated zone in the soil, a phenomenon ignored in many hydrologic models directed at predicting slope instability [e.g., *Iida*, 1984; *Okimura and Kawatani*, 1987; *Wu and Sidle*, 1995].

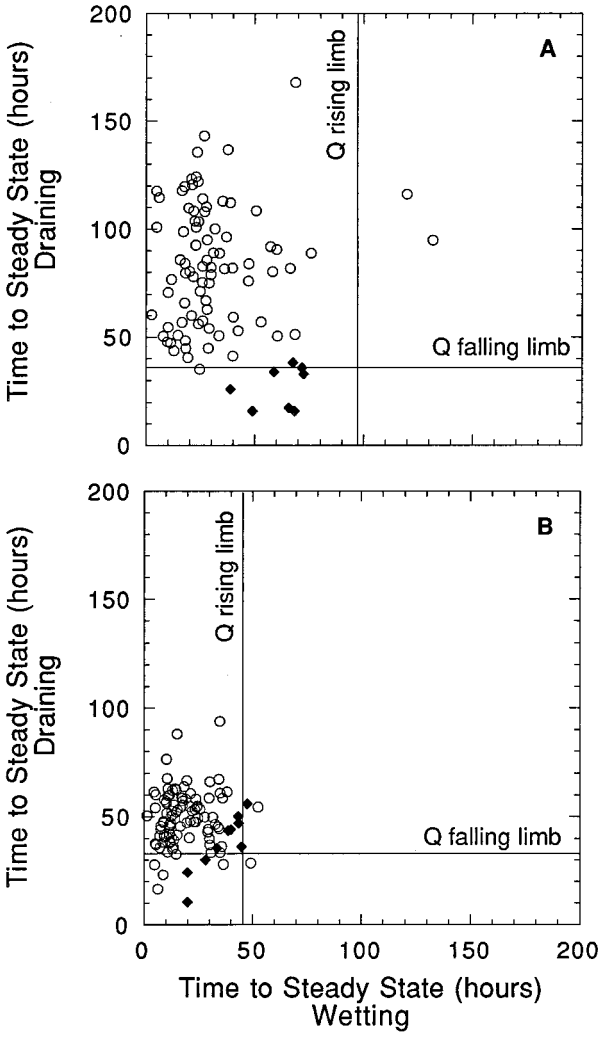

Figure 9. Steady state response field for unsaturated and saturated zones relative to the catchment runoff for experiments (a) 1 and (b) 2. Fields of possible response are created by the crossing of the falling and rising limb response of the discharge at the upper weir (labeled on graph). Piezometers are shown in black diamonds, and tensiometers are open circles.

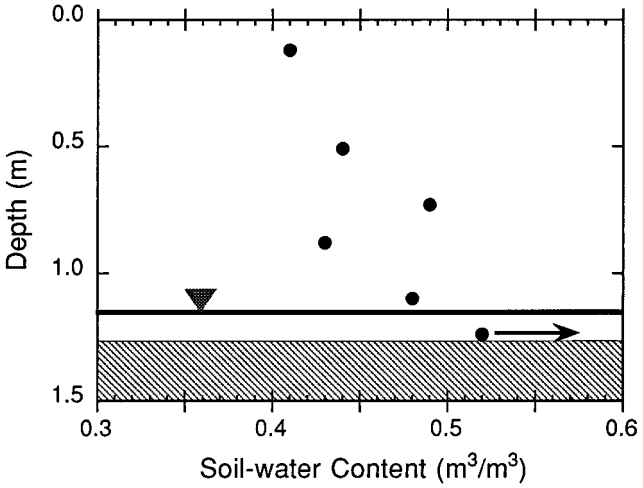

Figure 10. Soil-water content profile from the valley axis, along row 8, during the sixth day of experiment 1. The inverted triangle denotes the water table surface, and the shaded region represents the underlying bedrock. The saturated zone for water content is a minimum because some water was lost during sample recovery.

It is widely recognized that the size of storm needed to cause slope instability diminishes through the winter [e.g., *Keefer et al*., 1987; *Cannon and Ellen*, 1988; *Wilson and Wieczorek*, 1995]. While this effect is usually ascribed to increasing background-saturated conditions in the soil mass, the observations reported here suggest another mechanism. Early in the rainy season, the soil will respond to pulses of rain by increasing soil-water content. As soil-water content increases, the likelihood that pressure heads will attain near-zero values also increases, and pulses of rain can lead to a rapid displacement of preexisting soil-water to the saturated zone, causing rapid pore pressure rise there, expansion of the saturated zone, and slope instability. Hence the evolution of the unsaturated zone through the wet season and during particular storms may be as important as the development of the saturated zone. In fact, on steep slopes where drainage of the saturated zone can be fairly rapid, an important control on slope instability may be the rapid increase of unsaturated flux to the saturated zone, enabling pore pressures to rise significantly. This suggests that ignoring the influence of the unsaturated zone in slope stability modeling may lead to spurious results regarding analyses of frequency and magnitude of destabilizing rainfall.

6. Conclusions

Analysis of the hydrologic response to two sustained irrigation experiments on a steep, soil-mantled unchanneled valley

reveals that the unsaturated zone dynamics play a primary role in dictating the timing and magnitude of pore pressure response and discharge from the hillslope. We found that in response to irrigation, steady discharge and steady saturated zone pore pressures occur only after steady state develops in the unsaturated zone. Hence the lag time in the head field development in the unsaturated zone is an important time lag in the site response. However, we also found that the time to first response and time to steady state for tensiometers were faster than a simple plug flow approximation. Furthermore, a short period of rain during the end of experiment 2 revealed that the saturated zone response and peak discharge occurred much faster than expected by advection. These observations lead us to propose that a pressure wave which passed through the unsaturated zone undetected led to the relatively quick dynamic response of the site to incoming precipitation.

The single attribute that tends to dominate the hydrologic response of this catchment is the soil-water retention curve. The soil-water retention properties yield near-zero pressure heads throughout the soil profile for slight but persistent rain. Once the soil attained near-zero pressure head, the unsaturated zone, saturated zone, and discharge became delicately linked such that a sudden increase in rainfall intensity generated slight but rapidly advancing pressure waves that induced slight changes in head gradient and very large changes in hydraulic conductivity. These changes produced a rapid release of stored soil-water that increased the delivery rate of water to the underlying saturated zone, leading to increased pore pressures and discharge. Moreover, pressure wave transmission may be a requisite mechanism connecting the unsaturated and saturated zones in soils that may be near saturation. Hence the hydrologic response of the landscape to precipitation events is greatly influenced by the dynamics of the unsaturated zone.

Acknowledgments. This project was supported by the U.S. Department of Agriculture (i.e., Western Regional Research and MacIntire-Stennis Projects), the UC Berkeley College of Natural Resources (Dean's discretionary funds), NSF (EAR 8417467), USGS Water Resources Grant (14080001G2111), UC Berkeley Minority Fellowship Program, GSA Student Research Grant Program (4825-91), and the Weyerhaeuser Company. Tetsu K. Tokunaga gave technical assistance on experimental design. Wilford R. Gardner and James W. Kirchner offered critical comments throughout the data analyses and the development of this manuscript. Field data were acquired by David Brown, Mark Caruso, Darryl Granger, James W. Kirchner, Jeff Light, Deborah Lowenherz, Rita Rausch, Rohit Salve, Juan Somoano, and Kate Sullivan. Jim Clarke, Tom Hazard, and John Heffner provided logistical and technical support. Tor Roberts assisted with laboratory work. Comments by anonymous reviewers improved the clarity of this manuscript.

References

Andersen, L. J., and T. Sevel, Six years' environmental tritium profiles in the unsaturated and saturated zones, *Isot. Tech. Groundwater Hydrol*., *1*, 3–20, 1974.

Anderson, M. G., and T. P. Burt, The role of topography in controlling throughflow generation, *Earth Surf. Processes*, *3*, 331–344, 1978.

Anderson, S. P., Flow paths, solute sources, weathering and denudation rates: The chemical geomorphology of a small catchment, Ph.D. thesis, 380 pp., Univ. of Calif., Berkeley, 1995.

Anderson, S. P., W. E. Dietrich, D. R. Montgomery, R. Torres, M. E. Conrad, and K. Loague, Subsurface flow paths in a steep, unchanneled catchment, *Water Resour. Res*., *33*(12), 2637–2653, 1997a.

Anderson, S. P., W. E. Dietrich, R. Torres, D. R. Montgomery, and K. Loague, Concentration-discharge relationships in runoff from a steep, unchanneled catchment, *Water Resour. Res*., *33*(1), 211–225, 1997b.

Baldwin, E. M., Eocene stratigraphy of southwestern Oregon, *Bull. Oreg. Dep. Geol. Miner. Ind*., *83*, 1–38, 1974.

Benda, L., and T. Dunne, Stochastic forcing of sediment supply to channel networks from landsliding and debris flows, *Water Resour. Res*., *33*(12), 2849–2863, 1997.

Beven, K., and M. J. Kirkby, A physically based, variable contributing area model of basin hydrology, *Hydrol. Sci. Bull*., *24*(1), 43–69, 1979.

Camp, C. L., Excavations of burrows of the rodent *Aplodontia*, with observations on the habits of the animal, *Univ. Calif. Publ. Zoology*, *17*, 517–536, 1918.

Cannon, S. H., and S. D. Ellen, Rainfall that resulted in abundant debris-flow activity during the storm, in *Landslides, Floods, and Marine Effects of the Storm of January 3–5, 1982, in San Francisco Bay Region, California*, *U.S. Geol. Surv. Prof. Pap*., *1434*, 27–33, 1988.

Carsel, R. F., and R. S. Parrish, Developing joint probability distributions of soil water retention characteristics, *Water Resour. Res*., *24*(5), 755–769, 1988.

Cassel, D. K., and A. Klute, Water potential: Tensiometry, in *Methods of Soil Analysis*, *Part I: Physical and Mineralogical Methods*, edited by A. Klute, *SSSA Spec. Publ*., *9*, 563–596, 1986.

De Vries, J., and T. L. Chow, Hydrologic behavior of a forested mountain soil in coastal British Columbia, *Water Res. Res*., *14*(5), 935–942, 1978.

Dietrich, W. E., and T. Dunne, Sediment budget for a small catchment in a mountainous terrain, *Z. Geomorphol*., *Suppl*., *29*, 191–206, 1978.

Dietrich, W. E., C. J. Wilson, D. R. Montgomery, J. McKean, and R. Bauer, Erosion thresholds and land surface morphology, *Geology*, *20*(8), 675–679, 1992.

Dietrich, W. E., C. J. Wilson, D. R. Montgomery, and J. McKean, Analysis of erosion thresholds, channel networks, and landscape morphology using a digital terrain model, *J. Geol*., *101*(2), 259–278, 1993.

Dietrich, W. E., R. Reiss, M.-L. Hsu, and D. R. Montgomery, A process based model for colluvial soil depth and shallow landsliding using digital elevation data, *Hydrol. Processes*, *9*(3–4), 383–400, 1995.

Dunne, T., Field studies of hillslope flow processes, in *Hillslope Hydrology*, edited by M. J. Kirkby, pp. 227–294, John Wiley, New York, 1978.

Feldhamer, G. A., and J. A. Rochelle, Mountain beaver (*Aplodontia rufa*), in *Wild Mammals of North America*, edited by J. A. Chapman and G. A. Feldhamer, pp. 167–176, Johns Hopkins Univ. Press, Baltimore, Md., 1982.

Freeze, R. A., Role of subsurface flow in generating surface runoff, 2, Upstream source areas, *Water Resour. Res*., *8*(5), 1272–1283, 1972.

Gardner, W. R., Water movement below the root zone, *Trans. Int. Congr. Soil Sci. 8th*, *2*, 63–68, 1964.

Gilham, R. W., The capillary fringe and its effect on water-table response, *J. Hydrol*., *67*, 307–324, 1984.

Glass, R. J., and M. J. Nichol, Physics of gravity fingering of immiscible fluids with porous media: An overview of current understanding and selected complicating factors, *Geoderma*, *70*, 133–163, 1996.

Haagen, J. T., Soil survey of Coos County, Oregon, 269 pp., Soil Conservation Service, U.S. Dep. of Agric., Roseburg, Oreg., 1989.

Harr, R. D., Water flux in soil and subsoil on a steep forested slope, *J. Hydrol*., *33*, 37–58, 1977.

Hendrickx, J. M. H., L. W. Decker, and O. H. Boersma, Unstable wetting fronts in water repellent soils, *J. Environ. Qual*., *22*, 109–118, 1993.

Hewlett, J. D., Tracing storm and base flow to variable source areas on forested headwaters, *Tech. Rep. 2*, 21 pp., Univ. of Ga., Athens, 1969.

Hewlett, J. D., and A. R. Hibbert, Moisture and energy conditions within a sloping soil mass during drainage, *J. Geophys. Res*., *68*(4), 1081–1087, 1963.

Hewlett, J. D., and A. R. Hibbert, Factors affecting the response of small watersheds to precipitation in humid areas, in *Forest Hydrology*, edited by W. E. Sopper and H. W. Lull, pp. 275–290, Pergamon, New York, 1967.

Hill, D. E., and J.-Y. Parlange, Wetting front instability in layered soils, *Soil Sci. Soc. Am. Proc*., *36*, 697–702, 1972.

Horton, J. H., and R. H. Hawkins, Flow path of rain from the soil surface to the water table, *Soil Sci*., *100*(6), 377–383, 1965.

Horton, R. E., An approach toward the physical interpretation of infiltration-capacity, *Soil Sci. Soc. Am. Proc*., *5*, 399–417, 1940.

Hsu, M.-L., A grid based model for predicting soil depth and shallow landslides, Ph.D. thesis, 254 pp., Univ. of Calif., Berkeley, 1994.
Humphrey, N. F., Pore pressure in debris flow initiation, M.S. thesis, 169 pp., Univ. of Wash., Seattle, 1983.
Iida, T., A hydrological method of estimation of the topographic effect on the saturated through flow, *Trans. Jpn. Geomorphol. Union*, *5*, 1–12, 1984.
Kayane, I., and I. Kaihotsu, Some experimental results concerning rapid water table response to surface phenomena, *J. Hydrol*., *102*, 215–234, 1988.
Keefer, D. K., C. R. Wilson, R. K. Mark, E. E. Brabb, W. M. Brown, S. D. Ellen, E. L. Harp, G. F. Weiczorek, C. S. Elger, and R. S. Zatkin, Real time landslide warning during heavy rainfall, *Science*, *238*(4829), 921–925, 1987.
Luxmoore, R. J., Micro-, meso-, and macroporosity of soil, *Soil Sci. Soc. Am. J*., *45*, 671–672, 1981.
Luxmoore, R. J., and L. A. Ferrand, Towards pore scale analyses of preferential flow and chemical transport, in *Water Flow and Solute Transport in Soils*, edited by D. Russo, and G. Dagan, pp. 45–60, Springer-Verlag, New York, 1993.
Luxmoore, R. J., P. M. Jardine, G. V. Wilson, J. R. Jones, and L. W. Zelazny, Physical and chemical controls on preferred path flow through a forested hillslope, *Geoderma*, *46*, 139–154, 1990.
Marthaler, H. P., W. Vogelsanger, F. Richard, and P. J. Wieringa, A pressure transducer for field tensiometers, *Soil Sci. Soc. Am. J*., *47*(4), 624–627, 1983.
Marui, A., M. Yasuhara, K. Kuroda, and S. Takayama, Subsurface water movement and transmission of rainwater pressure through a clay layer, in *Hydrology of Warm Humid Regions*, *IAHS Publ*., *216*, 463–470, 1993.
McCord, J. T., D. B. Stephens, and J. L. Wilson, Hysteresis and state-dependent anisotropy in modeling unsaturated hillslope hydrologic processes, *Water Resour. Res*., *27*(7), 1501–1518, 1991.
McDonnell, J. J., A rationale for old water discharge through macropores in a steep, humid catchment, *Water Resour. Res*., *26*(11), 2821–2832, 1990.
Montgomery, D. R., Channel initiation and landscape evolution, Ph.D. thesis, 421 pp., Univ. of Calif., Berkeley, 1991.
Montgomery, D. R., and W. E. Dietrich, Where do channels begin?, *Nature*, *336*, 232–234, 1988.
Montgomery, D. R., and W. E. Dietrich, A physically based model for the topographic control on shallow landsliding, *Water Resour. Res*., *30*(4), 1153–1171, 1994.
Montgomery, D. R., W. E. Dietrich, R. Torres, S. P. Anderson, and K. Loague, Hydrologic response of a steep unchanneled valley to natural and applied rainfall, *Water Resour. Res*., *33*(1), 91–109, 1997.
Moore, I., E. M. O'Loughlin, and G. J. Burch, A contour based topographic model for hydrological and ecological applications, *Earth Surf. Processes Landforms*, *13*(4), 305–320, 1988.
Mosely, M. P., Streamflow generation in a forested watershed, New Zealand, *Water Resour. Res*., *15*(4), 795–806, 1979.
Mosely, M. P., Subsurface flow velocities through selected forest soils, South Island, New Zealand, *J. Hydrol*., *55*, 65–92, 1982.
Novakowski, K. S., and R. W. Gilham, Field investigations of the nature of water-table response to precipitation in shallow water-table environments, *J. Hydrol*., *97*, 23–32, 1988.
Okimura, T., and T. Kawatani, Mapping of the potential surface failure sites on granite mountain slopes, in *Proceedings of the First International Conference on Geomorphology*, *Part 1*, edited by V. Gardiner, pp. 131–138, Int. Assoc. Geomorphol., Manchester, England, 1987.
O'Loughlin, E. M., Prediction of surface saturation zones in natural catchments by topographic analysis, *Water Resour. Res*., *22*(5), 794–804, 1986.
Philip, J. R., Hillslope infiltration: Planar slopes, *Water Resour. Res*., *27*(1), 109–117, 1991.
Pierson, T. C., Piezometric response to rainstorms on forested hillslope drainage depressions, *N. Z. J. Hydrol*., *19*(1), 1–10, 1980.
Reneau, S. L., and W. E. Dietrich, Size and location of colluvial landslides in a steep forested landscape, *IAHS Publ*., *165*, 39–48, 1987.
Reynolds, W. D., and D. E. Elrick, In situ measurement of field-saturated hydraulic conductivity, sorptivity, and the α parameter using the Guelph Permeameter, *Soil Sci*., *140*, 292–296, 1985.
Shreve, R. L., Stream lengths and basin areas in topologically random channel networks, *J. Geol*., *77*(4), 397–414, 1969.
Skaling, W., TRASE: A product history, in *Advances in Measurement of Soil Physical Properties: Bringing Theory Into Practice*, edited by G. C. Topp, W. D. Reynolds, and R. E. Green, *SSSA Spec. Publ*., *30*, 169–185, 1992.
Smith, R. E., Approximate soil water movement by kinematic characteristics, *Soil Sci. Soc. Am. J*., *47*, 3–8, 1977.
Stephens, D. B., *Vadose Zone Hydrology*, p. 82, CRC Press, Boca Raton, Fla., 1996.
Tsuboyama, Y., R. C. Sidle, S. Noguchi, and I. Hosoda, Flow and solute transport through the soil matrix and macropores of a hillslope segment, *Water Resour. Res*., *30*(4), 879–880, 1994.
van Genuchten, M. T., A closed-form equation for predicting the hydraulic conductivity of unsaturated soils, *Soil Sci. Soc. Am. J*., *44*, 892–898, 1980.
Weyman, D. R., Measurements of the downslope flow of water in a soil, *J. Hydrol*., *20*, 267–288, 1973.
Wilson, G. V., and R. J. Luxmoore, Infiltration, macroporosity, and mesoporosity distributions in two forested watersheds, *Soil Sci. Soc. Am. J*., *52*, 329–335, 1988.
Wilson, G. V., P. M. Jardine, R. J. Luxmoore, and J. R. Jones, Hydrology of a forested hillslope during storm events, *Geoderma*, *46*, 119–138, 1990.
Wilson, G. V., P. M. Jardine, R. J. Luxmoore, L. W. Zelazny, D. A. Lietzke, and D. E. Todd, Hydrogeochemical processes controlling subsurface transport from an upper subcatchment of Walker Branch Watershed during storm events, 1, Hydrologic transport processes, *J. Hydrol*., *123*, 297–316, 1991.
Wilson, R. C., and G. F. Wieczorek, Rainfall thresholds for the initiation of debris flow at La Honda, California, *Environ. Eng. Geosci*., *1*(1), 11–27, 1995.
Wu, W., and R. C. Sidle, A distributed slope stability model for steep forested basins, *Water Resour. Res*., *31*(8), 2097–2110, 1995.
Yeh, T.-C., L. W. Gelhar, and A. L. Gutjahr, Stochastic analysis of unsaturated flow in heterogeneous soils, 3, Observations and applications, *Water Resour. Res*., *21*(4), 465–471, 1985.
Zaslavsky, D., and A. S. Rogowski, Hydrologic and morphologic implications of anisotropy and infiltration in soil profile development, *Soil Sci. Soc. Am. Proc*., *33*, 594–599, 1969.
Zaslavsky, D., and G. Sinai, Surface hydrology, I, Explanation of phenomena, *J. Hydraul. Div*., *Am. Soc. Civ. Eng*., *7*(HY1), 1–16, 1981a.
Zaslavsky, D., and G. Sinai, Surface Hydrology, III, Causes of lateral flow, *J. Hydraul. Div*., *Am. Soc. Civ. Eng*., *7*(HY1), 37–52, 1981b.
Zimmermann, U., K. O. Munnich, W. Roether, W. Kruetz, K. Schubach, and O. Siegel, Tracers determine movement of soil moisture and evapotranspiration, *Science*, *152*(3720), 346–347, 1966.

S. P. Anderson, Department of Earth Sciences and Institute of Tectonics, University of California, Santa Cruz, CA 95064-1077. (e-mail: spa@bagnold.ucsc.edu)

W. E. Dietrich, Department of Geology and Geophysics, University of California, Berkeley, CA 94720-4767. (e-mail: bill@geomorph.berkeley.edu)

K. Loague, Department of Geological and Environmental Sciences, Stanford University, Stanford, CA 94305-2115. (e-mail: keith@pangea.stanford.edu)

D. R. Montgomery, Department of Geological Sciences, University of Washington, Seattle, WA 98195. (e-mail: dave@bigdirt.geology.washington.edu)

R. Torres, Department of Geological Sciences, University of South Carolina, Columbia, SC 29208. (e-mail: torres@geol.sc.edu)

(Received March 4, 1997; revised February 19, 1998;
accepted April 3, 1998.)